The variability of the proximal femur in catarrhines – a new 3D method for describing anatomical structures

T. Pfisterer[1], F.L. Bookstein[1,2], B. Breuckmann[3], K. Schaefer[1], T.B. Viola[1], H. Woerner[3], H. Seidler[1].
[1] Department of Anthropology, University of Vienna, Austria, [2] Department of Statistics, University of Washington, Seattle, USA, [3] Breuckmann GmbH, Meersburg, Germany

A. Introduction

For a century physical anthropologists have quantified skeletal form using distances and angles measured directly on bones (Martin, 1914). Three dimensional digitizers make it easier to quantify extended three-dimensional structures, but still require physical access to the objects. There is some recent work on the femur (Harmon, 2005, Weaver, 2002) along these lines. On most postcranial structures, there are no Type I landmarks (histologically defined points, Bookstein, 1991) or in general, points that can be named are much less common and their definitions much more arbitrary than the analogues on the skull.

When information from surfaces is relevant to function, especially for postcranial applications, it may be better to extract information from surface form directly using new instruments such as 3D surface scanners. Here we present an application of these methods in the context of a study of form and locomotion in catarrhines.

B. Material

Our sample consists of 72 femurs from 10 species of catarrhines (Table 1), taxa marked with an asterisk comprise summarised species due to small sample size. The *H. sapiens* sample comprises 32 Khoi San of the Pöch collection, Department of Anthropology, Univeristy Vienna, and 12 Europeans (early medieval period) from Gars/Thunau from the collection of the Department of Anthropology, Natural History Museum, Vienna. All hominoids and cercopithecoids are from the Department of Vertebrate Zoology, Natural History Museum, Vienna. All specimens are adults, whenever possible the right femur was used, otherwise the left one was mirror-imaged in Rapidform.

Table 1. Number of specimens for each species and sex

Species	Males	Females	Indet.	Total
Homo sapiens	19	24	0	43
Pan troglodytes	3	2	1	6
Gorilla gorilla	4	3	0	7
Pongo pygmaeus	2	2	0	4
*Hylobates sp.**	0	0	3	3
Papio hamadryas	1	1	0	2
Erythrocebus patas	1	1	0	2
Theropithecus gelada	1	0	0	1
*Cercopithecus sp.**	3	1	0	4
Total	34	34	4	72

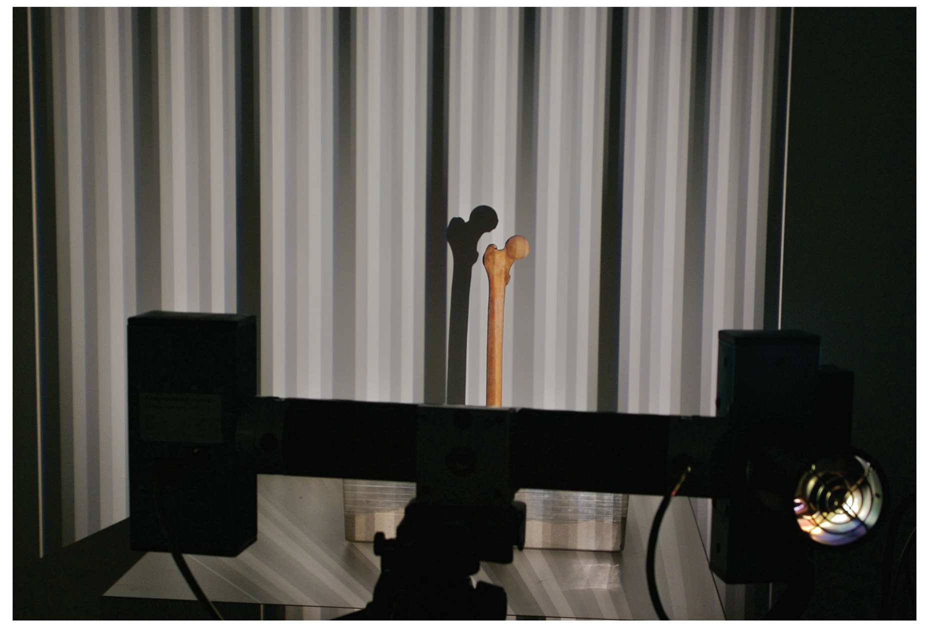

Figure 1. Facing the scanner from behind while projecting the Gray-code onto the femoral surface.

C. Methods

The surface data was collected by a Breuckmann triTOS surface scanner (http://www.breuckmann.com). This instrument gathers coordinate data by using structured illumination (projected stripe patterns, called Gray-code) (Figure 1) and phase shift, optically triangulated from several points of view. For the reconstruction algorithm, see Breuckmann, 1994.

Surfaces with strong relief, such as femurs in the vicinity of the fossa trochanterica, often are incomplete in single views owing to superimposition of structures. For the present application, the final surface reconstructions combined up to thirty single scans, totalling about one hour's machine time, followed by about thirty minutes for the preparation, alignment and merging of the resulting multiple images. Complete femoral surfaces involved up to 1.5 million surface triangles. The resolution and accuracy were both on the level of 70µ.

After scanning the work on the physical specimen is completed. The post-processing steps were done in the Breuckmann software optoCAT (Version 4.01.08) and in the program Rapidform (version rapidform2006SP1, INUS Technology, Inc.). We manually removed vertices unreliable due to acquisition errors, deleted overlapping and non-manifold areas, crossing triangles and filled the remaining holes by spline interpolation. All femurs were cut off at 35% of their total length.

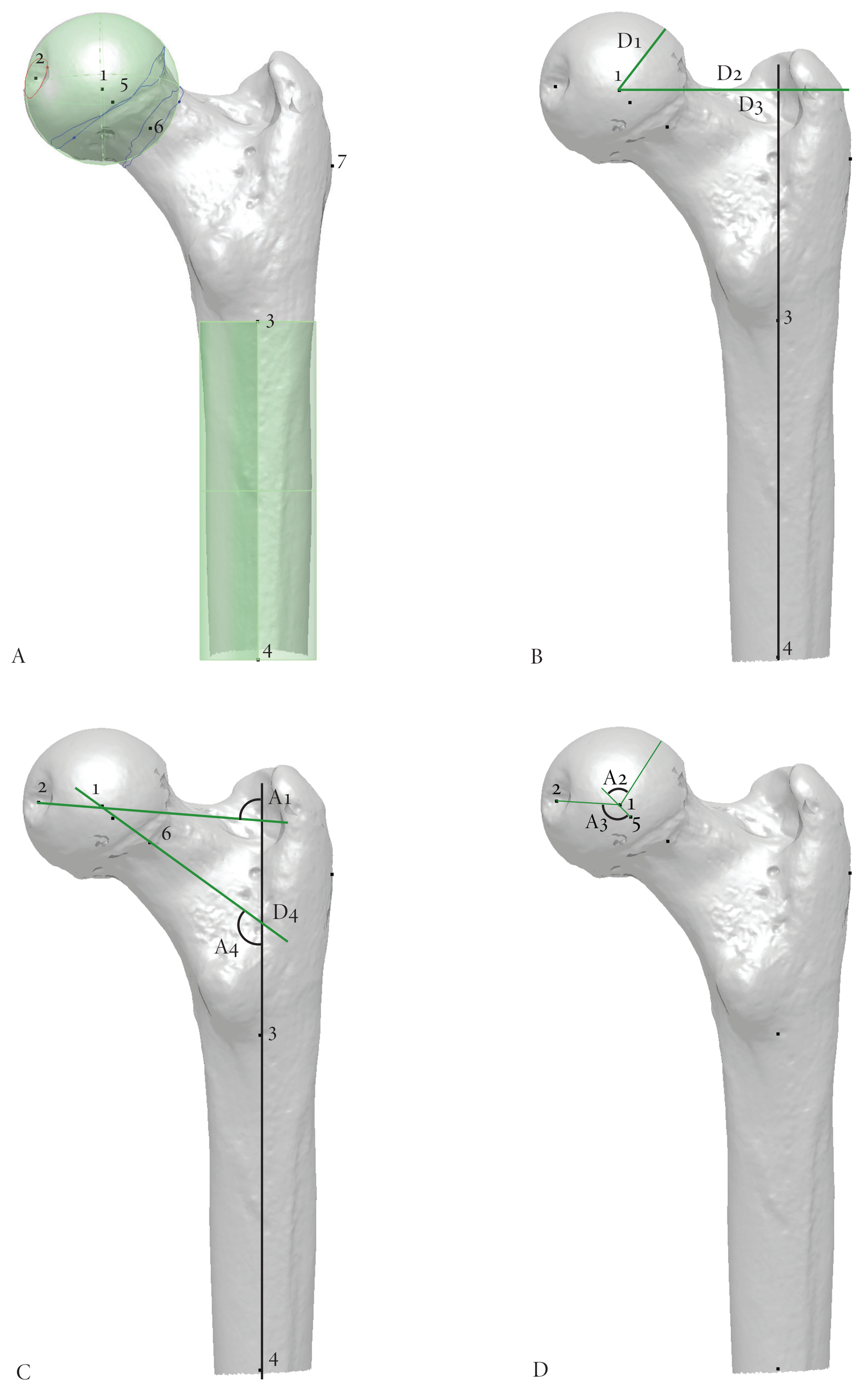

Figure 2. Upper row shows how points were constructed via fitting geometrical objects (A) into the femur and (B) displays all distances which were computed. Lower row: shows all the angles (C, D) which were constructed between all points and landmarks.

Table 2. Landmarks and auxilliary points used

Points	Definition
1. Centre of the femoral head	Centre of a sphere fitted to the articular surface
2. Centroid of the *Fovea capitis femoris*	Centroid of a curve drawn around the *Fovea capitis femoris*
3. Proximal shaft centre*	Top center of a cylinder fit to the shaft between the lesser trochanter and 30% of femoral length
4. Distal shaft centre*	Bottom center of the cylinder
5. Centroid of the articular surface margin	Centroid of a curve delimiting the articular surface
6. Centre of the femoral neck*	Centroid of the section through the neck at the smallest breadth in posterior view, construction is dependent on orientation of the femur (after Martin, 1914)
7. Lateralmost point of the greater trochanter*	Most lateral point on the *Trochanter maior*

Table 3. Measurements used

	Measurements	Definitions
Angles		
A1	fovea.body.angle	angle between the vectors Point 1-2 to Pt 3-4
A2	artic.angle	Angle described by the cosine of the distance Pt1-5 and to radius
A3	fovea.head.angle	angle between the vectors Pt 1-2 to Pt 1-5
A4	collo.diaphyseal.angle	angle between the vectors Pt1-6 and Pt3-4
Distances		
D1	radius	Radius of the sphere fitted to the femoral head
D2	dist.head.body	Minimal distance between the vector Pt 3-4 and the vector Pt 1-6
D3	dist.head.axis	Distance between Pt 1 and the shaft axis, perpedicular to the shaft axis
D4	dist.trochanter.action	Projected distance between Pt1 and the most lateral point on the greater trochanter, perpendicular to the shaft axis (Leverage arm of gluteal muscles)
Area		
	articular.surf.area	Area of the articular surface

D. Landmarks, distances and angles

Landmarks were generated in Rapidform by using a custom macro by fitting geometrical objects to the surface (Figure 2). The advantage of using this program and surface scans is that one can always go back and take new points or correct errors.

Landmarks 1, 2 and 5 are true landmarks (Table 2) all of Bookstein Type III (summaries of information at a distance). There are also four "pseudo-landmarks" (or auxiliary points) (marked with an asterisk) functioning purely to supply information for measurements of distances or angles, namely, point 3 and 4 along the shaft axis (to describe the shaft direction; by fitting a cylinder to the shaft), point 7 the most lateral point on the trochanter (for measurement of the action of the gluteus minimus muscle around the hip joint), and a "midpoint" of the neck computed in a specific view to accord with the classic definition of the collo-diaphyseal-angle (see Martin, 1914).

Additional information, that can only be gathered using this method, like the area of the articular surface (as delimited by the curve used for defining Point 5) was also collected, but not used in the present analysis.

We do not carry out any Procrustes analysis of point configurations, as there are not enough landmarks and, in any case, that analysis would be completely oblivious to the biomechanics of locomotion that is our ultimate research interest. Instead of using coordinates of points we constructed four distances and four angles (Table 3).

For the purpose of this preliminary demonstration, lacking the necessary mass information for scaling or other mechanical studies, we simply treat these data by the methods of classic "multivariate morphometrics", in an ordination by principal components of standardized variables.

Table 4. Means of all variables for each species

Species	n	Dist.head. axis (mm)	Dist. troch. action (mm)	Radius (mm)	Dist.head. body (mm)	Neck.shaft. angle	Artic. angle	Art. surface area (mm²)
Homo sapiens	43	35.7	56.2	19.4	5.4	125.4°	103.2°	3018.8
South Africans	31	35.7	56.2	19.4	5.4	125.4°	103.2°	3018.8
Europeans	12	45.1	69.9	23.6	7.2	120.6°	98.4°	4097.1
Gorilla gorilla	7	43.1	67.4	23.1	4.4	124.6°	98.9°	4032.6
*Hylobates sp.**	3	13.7	19.1	6.9	0.8	123.6°	103.9°	384.5
Pan troglodytes	6	30.4	48.4	16.5	1.5	126.4°	101.1°	2123.9
Pongo pygmaeus	4	23.8	43.3	17.1	4.9	141.8°	110.1°	2541.3
*Cercopithecus sp.**	4	15.65	22.8	6.95	0.95	100.25°	104.75°	398.3
Erythrocebus patas	2	19.2	28.7	7.5	0.8	104.5°	113.7°	504.7
Papio hamadryas	2	20.2	31.9	10.1	1.1	106.6°	103.6°	833.8
Theropithecus gelada	1	21.9	35.2	10.9	2.4	106.3°	97.5°	893.4

E. Results and Discussion

The biplot Figure 3 shows that all the distances are correlated with each other and that they are independent from the angles. Figure 4 shows the separation between the species along the first principal component, which represents size. Figure 5 demonstrates that except *Gorilla*, which exposes a great sexual dimorphism, sexual dimorphism can not be detected, probably due to the small sample size.

We have demonstrated a very useful compromise between the classical way of distance/angle measurements and the modern context of image-driven "virtual anthropology" whereby a very high-dimensional data representation supports the very sparse selection of "important" measurements known a-priori from previous work.

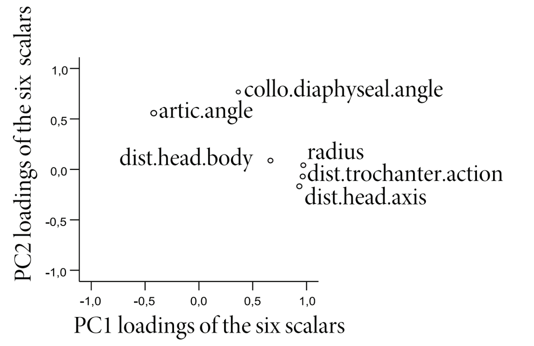

Figure 3. Shows the loadings of the scalars from the PCA, all distance variables are correlated.

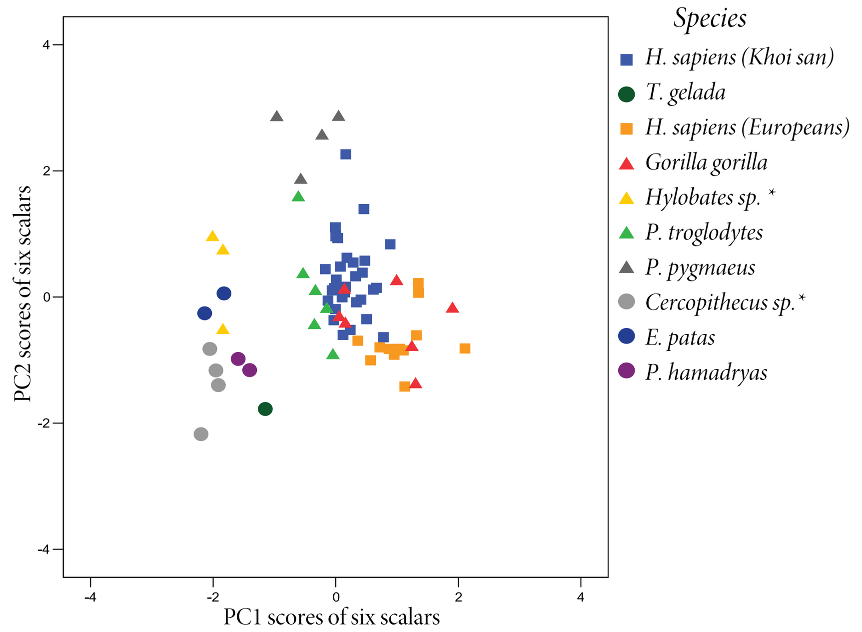

Figure 4. Shows the separation of the species along the principal components 1 and 2 (species * were summarised for the analysis due to the small sample size).

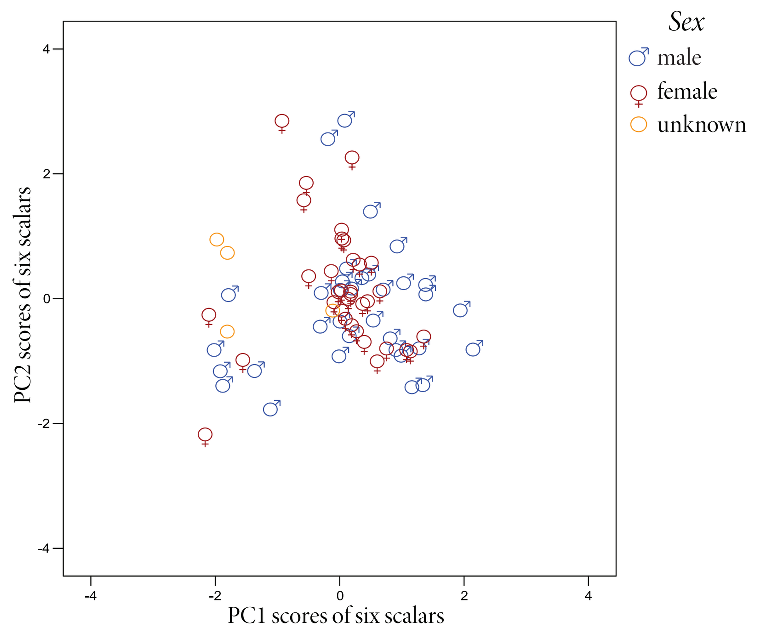

Figure 5. Due to the small sample size it is not possible to separate most of the species by sex.

F. Limitations

- The scanner used has its problems when the underlying geometric or optical assumptions are violated. For example, specular reflections, and stray light (shiny spots), fractal regions of the surface (e.g. at sites of breakage), surface patches that are actually black (the same colour as the stripes), and reflective aspects of the image background all cause problems, mostly consisting of holes in the resulting mesh.
- The Rapidform software package was not designed for such biological applications but works well. A disadvantage is the high price of this, and other comparable software packages. Freeware alternatives would be of great use, but are not yet available.
- There are limitations in defining new landmarks, which can be constructed via geometrical objects and are homologous, because of the complicated shape of the femur. The greater and lesser trochanters, for example can not be described easily.

G. Advantages

- The specimens are virtual, not real allowing one to go back to the surface representations over and over to collect additional geometric information as suggested by new literature, preliminary findings, or insights from colleagues. We already used this advantage to generate new points.
- Surfaces can be averaged, thereby making possible the reconstruction of broken or otherwise incomplete specimens, and can be represented by semilandmarks instead of distances and angles when the topic is one of systematics rather than functional morphology.

References

Bookstein, F. L. (1991). Morphometric tools for landmark data geometry and biology. New York, Cambridge (UK): Cambridge University Press.
Breuckmann, B., Halbauer, F., Klaas, E., Winterberg, H. (1994). Industrielle Praxis der topometrischen 3D-Messtechnik. In GMA-Bericht 23 – Optisches Messen von Länge und Gestalt – Erfahrungsaustausch zwischen Anwendern und Entwicklern, Düsseldorf.
Breuckmann GmbH. (2005) *opto*CAT 4.01.08. Breuckmann GmbH, Meersburg, Germany.
Harmon, E. H. (2006). Size and shape variation in *Australopithecus afarensis* proximal femora. Journal of Human Evolution 51.
Harmon, E. H. (2005). A comparative analysis of femoral morphology in *Australopithecus afarensis*: implications for the evolution of bipedal locomotion. PhD thesis, Department of Anthropology, Arizona State University.
INUS Technology, Inc. (2006). Rapidform 2006 SP1. INUS Technology, Inc. Seoul, South Korea.
Martin, R. (1914). Lehrbuch der Anthropologie in systematischer Darstellung – mit Berücksichtigung der anthropologischen Methoden. Jena, Verlag von Gustav Fischer.
Weaver, T. D. (2003). A multi-causal functional analysis of hominid hip morphology. PhD thesis, Department of Anthropological Sciences, Standford University.

Acknowledgements

This work was supported by the grant GZ200.093/I-VI/2004 (PI H. Seidler) from the Austrian Council for Science and Technology and the EU PF4 Marie Curie Actions grant (EVAN, Human Resource and Mobility Activity) MRTN-CT-2005-019564. We thank Maria Teschler-Nicola and Barbara Herzig for access to the collections of the Natural History Museum, Vienna.